Histopathological Correlates of Global and Segmental Left Ventricular Systolic Dysfunction in Experimental Chronic Chagas Cardiomyopathy

Luciano Fonseca Lemos de Oliveira, PT, Ms; Minna Moreira Dias Romano, MD, PhD; Eduardo Elias Vieira de Carvalho, PT, Ms; Jorge Mejia Cabeza, PhD; Hélio Cesar Salgado, MD, PhD; Rubens Fazan Júnior, MD, PhD; Renata Sesti Costa, PhD; João Santana da Silva, PhD; Maria de Lourdes Higuchi, MD, PhD; Benedito Carlos Maciel, MD, PhD; Edécio Cunha-Neto, MD, PhD; José Antônio Marin-Neto, MD, PhD; Marcus Vinícius Simões, MD, PhD

Background—Chronic Chagas cardiomyopathy in humans is characterized by segmental left ventricular wall motion abnormalities (WMA), mainly in the early stages of disease. This study aimed at investigating the detection of WMA and its correlation with the underlying histopathological changes in a chronic Chagas cardiomyopathy model in hamsters.

Methods and Results—Female Syrian hamsters (n=34) infected with 3.5×10^4 or 10^5 blood trypomastigote *Trypanosoma cruzi* (Y strain) forms and an uninfected control group (n=7) were investigated. After 6 or 10 months after the infection, the animals were submitted to in vivo evaluation of global and segmental left ventricular systolic function by echocardiography, followed by euthanasia and histological analysis for quantitative assessment of fibrosis and inflammation with tissue sampling in locations coinciding with the left ventricular wall segmentation employed at the in vivo echocardiographic evaluation. Ten of the 34 infected animals (29%) showed reduced left ventricular ejection fraction (<73%). Left ventricular ejection fraction was more negatively correlated with the intensity of inflammation ($r=-0.63$; $P<0.0001$) than with the extent of fibrosis ($r=-0.36$; $P=0.036$). Among the 24 animals with preserved left ventricular ejection fraction (82.9±5.5%), 8 (33%) showed segmental WMA predominating in the apical, inferior, and posterolateral segments. The segments exhibiting WMA, in comparison to those with normal wall motion, showed a greater extent of fibrosis (9.3±5.7% and 7±6.3%, $P<0.0001$) and an even greater intensity of inflammation (218.0±111.6 and 124.5±84.8 nuclei/mm², $P<0.0001$).

Conclusions—Isolated WMA with preserved global systolic left ventricular function is frequently found in Syrian hamsters with experimental chronic Chagas cardiomyopathy whose underlying histopathological features are mainly inflammatory. (***J Am Heart Assoc.*** 2016;5:e002786 doi: 10.1161/JAHA.115.002786)

Key Words: Chagas heart failure • echocardiography • pathology

Chronic Chagas cardiomyopathy (CCC) is a significant cause of morbidity and mortality in Central and South America, with estimates of about 8 to 10 million infected people and 25 million people at risk.[1] Moreover, migratory currents have caused the spread of the disease, with thousands of infected people identified in the United States[2] and Europe.[3–5]

Despite its relevance, several clinical and pathophysiological aspects of CCC progression remain unknown, mainly due to the lack of long-term clinical cohort studies. The main aspect preventing the execution of these studies is the very long time period, about 3 decades, usually elapsing between the initial asymptomatic acute phase and the late chronic phase in which myocardial dysfunction and a dilated cardiomyopathy pattern become manifest.[6] Considering this scenario, appropriate animal models of CCC may constitute a relevant tool to investigate the mechanisms leading to chronic myocardial damage in this disease.[7–9]

An experimental model of chronic *Trypanosoma cruzi* infection in Syrian hamsters has been described, which mimics human CCC in many aspects,[10,11] including progressive left ventricular (LV) systolic dysfunction and dilation starting about 4 months after *T. cruzi* inoculation.[12,13]

Segmental LV wall motion abnormalities (WMA) are a conspicuous finding in human CCC.[14] In fact, several clinical studies have shown that LV regional WMA in the posterolateral and apical segments are very common and represent early findings in CCC, preceding the global LV dysfunction and dilation.[15,16] Although the prognostic meaning of these early abnormalities has not been defined, a retrospective study, comparing echocardiographic data from 2 examinations separated by an average of 5 years, suggested that early regional LV wall motion impairment was associated with more severe LV dysfunction at later stages.[17] The WMA in CCC have been classically interpreted as related to areas of regional fibrosis, even though no previous study has demonstrated this histopathological correlation. Also, no study addressed the investigation of regional LV systolic dysfunction in experimental models of CCC in hamsters.

The detection of LV regional dysfunction in animal studies could provide an opportunity to investigate the nature of histopathological changes underlying regional LV dysfunction in CCC, thus contributing to the understanding of the disease pathogenesis.

The objective of the present study was to investigate the presence of regional LV wall motion disturbances in a model of CCC in the Syrian hamster using high-resolution echocardiographic imaging, and to analyze the histopathological changes topographically related to these abnormalities. Additionally, we also intended to correlate quantitatively global LV dysfunction with the quantitative assessment of inflammation and fibrosis.

Materials and Methods

Experimental Animals

Twelve-week-old female hamsters (*Mesocricetus auratus*) used for the experiments were obtained from Anilab (Animais de Laboratório Criação e Comércio Ltda, Paulínia/SP, Brasil). The animals were kept in a climatically controlled environment, with free access to water and standard chow and under a 12-hour light/dark cycle.

Sixty animals were inoculated intraperitoneally with 3.5×10^4 (n=30) to 10^5 (n=30) blood trypomastigote forms of *T. cruzi*, Y strain. A control group of 8 animals received a saline inoculum of equal volume administered through the same route as used in the animals infected with *T. cruzi*.

The animals were submitted to all procedures under anesthesia with pentobarbital sodium (50 mg/kg) in order to avoid stress and pain. The study was approved by the Research Committee on Animal Experimentation of the Medical School of Ribeirão Preto of the University of São Paulo (protocol no. 034/2011).

General Study Design

After experimental infection with *T. cruzi*, the animals were observed in order to confirm infection by direct detection and count of circulating parasites and animal survival. The animals were followed for 6 (n=28) and 10 months (n=6) after infection and the survivors were submitted to the imaging studies. These time points after infection, as well as the number of *T. cruzi* inoculated, were chosen in order to obtain animals in the chronic phase of the disease exhibiting various degrees of ventricular dysfunction according to the observations reported by Bilate et al.[12] At the end of the study period, the animals were submitted to echocardiography followed by euthanasia and heart collection for histological analysis.

Echocardiogram

After sedation with an intraperitoneal injection of pentobarbital sodium (50 mg/kg), the anterior region of the animals' chest was depilated using a human commercial depilatory cream. The animals were positioned in left lateral decubitus under spontaneous ventilation and a Doppler ECG was obtained with a high-resolution Philips HD11XE 2-dimensional echocardiography system (Best, DA, Netherlands) equipped with a linear 15 MHz transducer. The parasternal window was used to obtain long- and short-axis LV images, the latter at the basal and middle (papillary) level. Different from clinical studies, in which the apical wall motion is assessed by using an apical view, in this study the apical region was evaluated in the long-axis parasternal view. M-mode images were obtained at the papillary level to measure the thickness of the interventricular septum and of the posterior LV wall and to determine the systolic and diastolic chamber dimensions.

The images obtained were recorded for offline data analysis at the end of the study. The images were obtained and analyzed by an observer who was experienced in obtaining and analyzing small-animal echocardiography, and who was blinded to the animal study group. The LV dimensions acquired in M-mode (short-axis images) during diastole and systole were used to determine the ejection fraction (EF) by the method of Teichholz.

Each measurement represented the mean of at least 5 consecutive cardiac cycles in the same projection, transducer position, and angulation and on the same frame of the frozen image.

LV systolic segmental wall motion was analyzed using a 13-segment model[18] in which the apex is evaluated on a long-axis image starting from the parasternal projection. A parasternal projection of the long axis and 2 short-axis section levels (basal and midventricular) of the LV were used

for segmentation (Figure 1A). Segmental wall motion was graded visually on each segment as 1=normal, 2=hypokinetic, and 3=akinetic/dyskinetic. The global segmental wall motion score was determined as the sum of the indices for each segment divided by the total number of segments.

Histopathology Methods

Under anesthesia with pentobarbital sodium (50 mg/kg), the animals were euthanized by opening of the chest, with the heart being rapidly excised and washed with PBS. Heart tissue samples were fixed in 10% formaldehyde for 24 hours and then transferred to 70% alcohol. The samples were progressively dehydrated, embedded in paraffin, cut, and stained with hematoxylin–eosin and picrosirius red for the quantitation of inflammation and fibrosis, respectively. Histopathological analysis was carried out on sections obtained at 3 levels of the heart (basal, midventricular, and apical). The sampling regions were chosen according to the same myocardial segmentation of the LV wall as used in the analyses of the in vivo echocardiography images in order to permit a topographic correlation between echocardiography and histology findings.

Histology Analysis

The slices were scanned with a digital image analysis system consisting of a digital scanner (Scanscope CS System; Aperio Technologies. Inc, Vista, CA) equipped with an Olympus UPlanSApo ×20 objective. The digitized images were analyzed with the Aperio ImageScope View Software (Aperio Technologies).
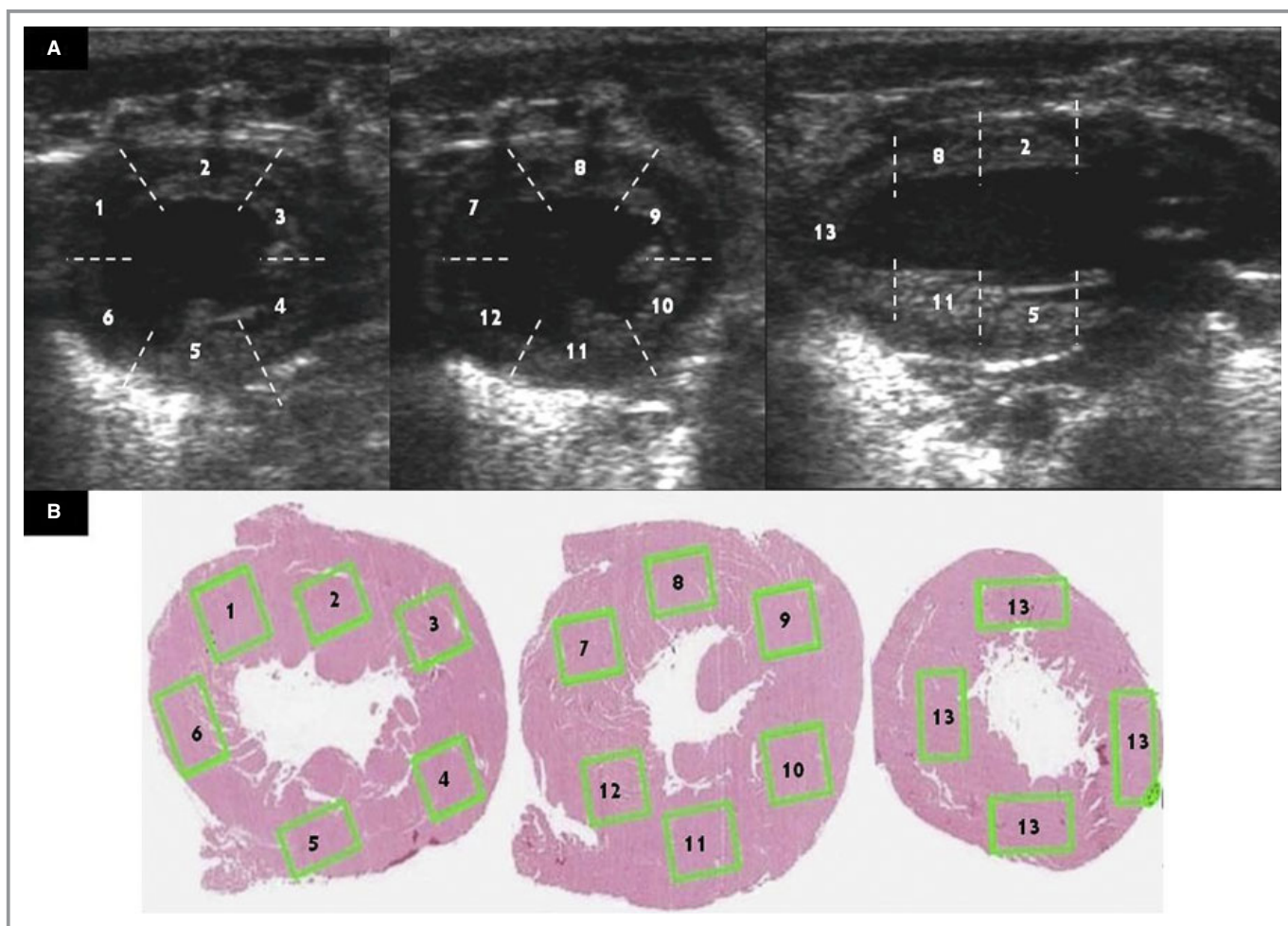

Figure 1. Illustrative examples of echocardiographic (A) and histological (B) images obtained at different levels of the LV cavity: basal (left images), midventricular (middle images), and apical (right images). The analysis fields depicted in the histopathological slices were topographically correlated with the LV wall segments of the in vivo images. The apex in the echocardiogram was evaluated in a parasternal long-axis image, while in the histological analysis an average of 4 sampling points in the apical slice was used. 1=basal anteroseptal, 2=basal anterior, 3=basal anterolateral, 4=basal posterolateral, 5=basal inferior, 6=basal inferoseptal, 7=mid-anteroseptal, 8=mid-anterior, 9=mid-anterolateral, 10=mid-posterolateral, 11=mid-inferior, 12=mid-inferoseptal, and 13=apex. LV indicates left ventricular.

Hematoxylin–eosin staining was used for descriptive qualitative analysis of the extent of tissue injury by an experienced pathologist who was blind to the group to which the animal belonged. Mononucleated cells with nucleus area of 10 to 50 μm^2 were identified and counted for quantitative analysis of inflammation using hematoxylin–eosin staining, thus permitting the determination of the extent of inflammatory infiltrates. The extent of fibrosis per mm^2 in relation to the total area analyzed was determined in the picrosirius red–stained samples.

A sampling area ranging from 1.5 to 2 mm^2 was used for each myocardial segment with the topographic correlation being maintained in regard to the same myocardial segments identified in in vivo imaging examinations (Figure 1B).

Statistical Analysis

Continuous variable data are reported as mean±SD and nominal variable data are reported as absolute (n) and relative (%) frequency.

The normal distribution of the variables was determined by the Kolmogorov–Smirnov test. The Student *t* test was used to determine the difference between the means of 2 groups for variables with normal distribution and homogenous variance. The Mann–Whitney test was used for variables with non-normal distribution. For simultaneous comparative analysis of 3 or more groups, 1-way ANOVA with Tukey's post-test was used for variables with normal distribution and the Kruskal–Wallis test, with Dunn's post-test, for variables with non-normal distribution. Linear regression and correlation analysis was performed by using the least-squares method, including the multiple regression analysis.

All analyses were carried out with the aid of the GraphPad InStat software, version 3.05, with the level of significance for differences set at 5% (*P*<0.05).

Results

Mortality

Overall mortality of the infected animals was 43% throughout the acute (33%) and chronic (10%) phases. Thus, a sample of 34 surviving infected animals was submitted to the echocardiography study. The animals infected with 3.5×10^4 infecting forms presented a mortality rate of 33%, which was lower than the mortality rate observed in the group with 10^5 infecting forms (53%), but not reaching statistical significance.

One control animal died as a consequence of anesthesia during the imaging examinations. Thus, at the end of the protocol the control group consisted of 7 animals.

Histopathological Changes—Qualitative Analysis

A qualitative analysis of histopathological data revealed multifocal myocarditis consisting of a mononuclear infiltrate, with fiber degeneration and myocytolytic lesions of varying intensity associated with a discrete increase of interstitial and perivascular fibrosis (Figure 2). However, there were no coalescent areas of fibrosis involving a significant extent of the LV wall. The histological changes were more intense in the animals with ventricular dysfunction and dilation compared to those with normal LVEF.

Analysis of Global Systolic Function and LV Remodeling

Echocardiographic LV assessment of control animals allowed the determination of the lower limit value for LVEF at 73%, defined by subtracting 2 SD from the mean value observed (81.9±4.6%). No change in LV wall motion was observed in this group.

Eighteen of the 34 animals investigated (53%) showed abnormal LV function. Among them, LV dysfunction was exclusively segmental in 8 (24%), whereas global systolic dysfunction (LVEF <73%) was detected in 10 (29%). All animals with reduced LVEF showed diffuse wall motion impairment (Figure 3).

The mean EF of the animals with global systolic dysfunction was 48.5±11.4% (ranging from 35.7% to 65.5%), a significantly lower value compared to control (81.9±4.6%, *P*<0.0001), The animals with reduced LVEF exhibited an increased LV end-diastolic diameter (0.62±0.14 cm) and wall motion score (1.7±0.5, *P*<0.0001) compared to control animals (0.44±0.04 cm, *P*=0.0003; and 1.0±0.0, respectively; Table).

Correlation between global LV systolic function and quantitative histological disturbances

Quantitative histopathological assessment of the animals classified according to the LV systolic function (Figure 4) revealed a significant difference in the number of inflammatory cells between the animals with reduced LVEF (224.8±86 nuclei/mm^2) and the remaining animals (control=113.2± 38.8; infected with preserved LVEF=107.7±43 nuclei/mm^2; *P*<0.0001). A significant difference in the extent of fibrosis was detected only between the control animals and the animals with reduced LVEF (4.5±1.8; 9.5±4.3%/mm^2, *P*=0.04).

A moderate negative correlation between LVEF and intensity of inflammation (*R*=−0.63; *P*<0.0001) was observed in the infected animals, as well as a weak negative correlation with the extent of fibrosis (*R*=−0.36; *P*=0.036), as shown in Figure 5. Multiple regression analysis revealed that the extent of inflammation (*P*=0.0007), but not the fibrosis (*P*=0.89),
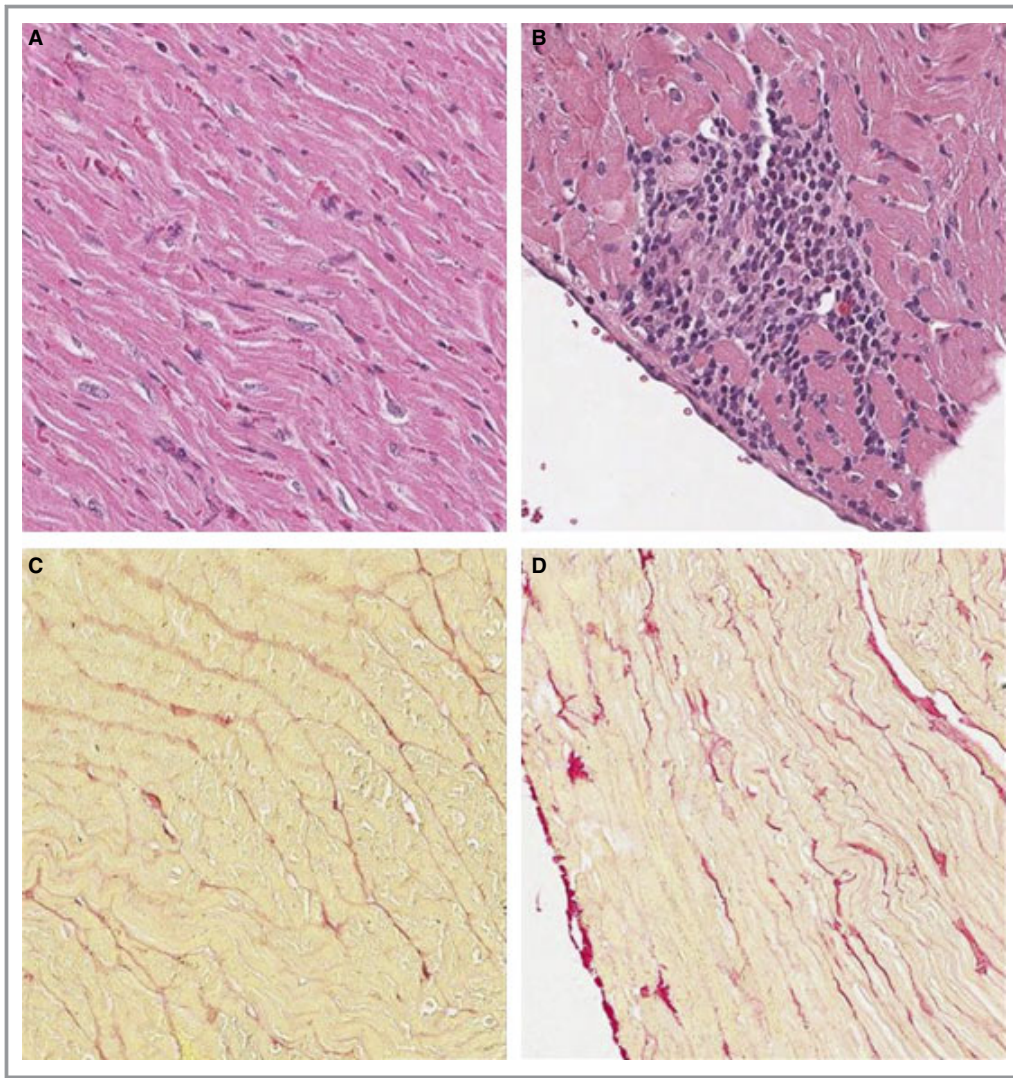
Figure 2. Illustrative examples of histopathological sections stained with hematoxylin-eosin (A and B) and picrosirius red (C and D) of an infected animal without LV dysfunction or dilation (A and C), and of an animal with global systolic LV dysfunction (B and D), which shows increased interstitial fibrosis and conspicuous focus of mononuclear inflammatory infiltrate. LV indicates left ventricular.

correlate in an independent manner with LVEF in the multiple regression model (R=0.63, P=0.0003).

Analysis of segmental LV systolic dysfunction

LV dysfunction was exclusively segmental in 8 of the 34 animals studied (24%). In 10 (29%) other animals diffuse WMA was associated with global systolic dysfunction. Thus, segmental parietal dysfunction involved 101 of the 234 segments analyzed (43%) in the 18 animals exhibiting this abnormality.

The apical region was the most affected myocardial region, being involved in 100% of the 18 animals with WMA and being akinetic in 8 (44%) and hypokinetic in 10 (56%). However, no typical LV apical aneurysm was identified (Figure 6).

Other segments preferentially involved were the inferior segment in 8 animals (44%) and the posterolateral segment in 10 (56%), and in both regions hypokinesis occurred.

Correlation between disturbances in segmental parietal mobility and histological findings

Considering the population of infected animals as a whole (n=34), histological analysis was possible in 438 of the 442 segments, since 4 segments showed artifacts during histological preparation and were excluded from the analysis.

The segments with reduced parietal mobility (n=101) showed a greater extent of fibrosis when compared to the segments with normal parietal mobility (n=337) (9.3±5.7% and 7.0±6.3%, respectively, P<0.0001) and a greater inten-
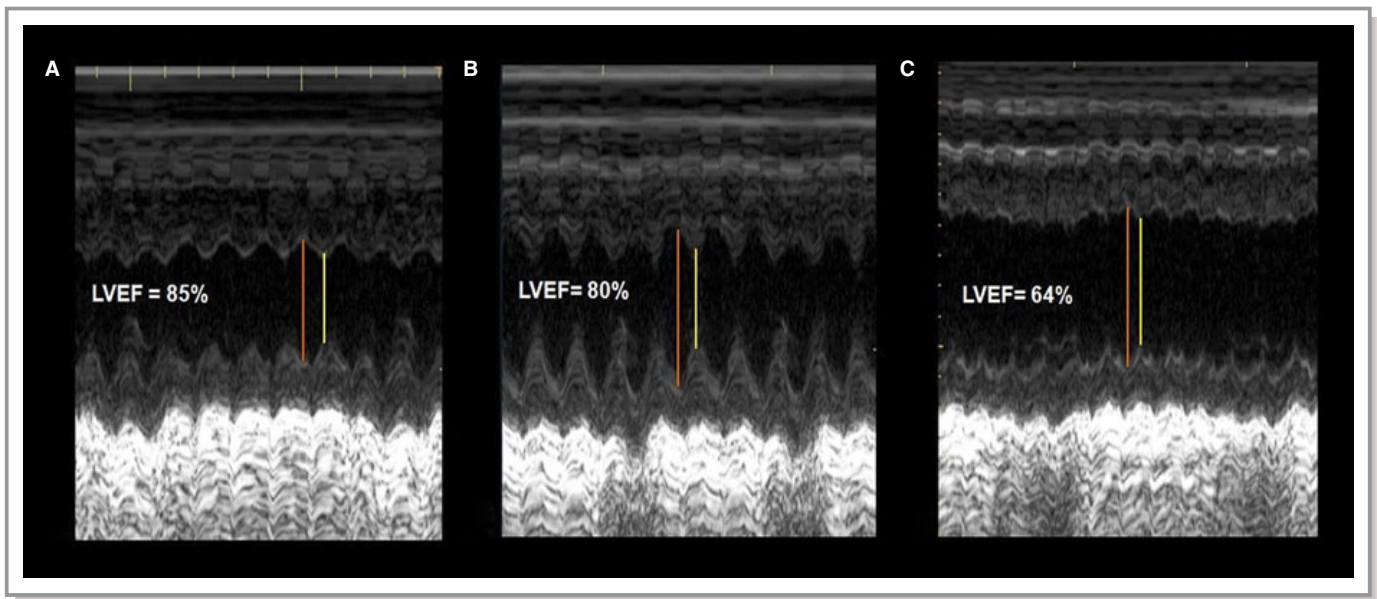
Figure 3. Representative images of M-mode echocardiography illustrating the LV dimensions used for the calculations of LVEF. The red and yellow lines represent the LV end-diastolic and systolic dimensions, respectively. A, Animal of the control group; (B) animal of the infected group with preserved EF; (C) animal of the infected group with reduced LVEF. EF indicates ejection fraction; LV, left ventricular.

sity of inflammation (218.0 ± 111.6 and 124.5 ± 84.8 nuclei/ mm^2, $P<0.0001$) (Figure 7).

In addition, individual wall motion scores showed a significant negative correlation with the intensity of inflammation ($r=0.53$, $P=0.0014$), but not with myocardial fibrosis ($r=0.25$, $P=0.16$).

Cardiac changes according to the parasite loads

Regarding the initial parasite load, the animals infected with 3.5×10^4 (n=20) infecting forms when compared to animals

Table. Summarized Echocardiogram Data for the Animals Classified According to LV Systolic Function

Groups	LVEF	LVEDD	LVSD	SCORE
Control (n=7)	81.9±4.6	0.44±0.04	0.24±0.04	1±0
Preserved LVEF (n=24)	82.9±5.5	0.49±0.08	0.26±0.06	1.04±0.07
Reduced LVEF (n=10)	48.5±11.4*	0.62±0.14†	0.49±0.13*	1.7±0.5*
P Value	<0.0001	0.0003	<0.0001	<0.0001

Data were analyzed statistically by ANOVA for multiple comparisons of the means. Data are reported as means±SD. LVEDD indicates left ventricular end-diastolic diameter; LVEF, left ventricular ejection fraction; LVSD, left ventricular end-systolic diameter; SCORE, left ventricular segmental parietal mobility score.
*$P<0.001$ vs control and preserved LVEF.
†$P<0.01$ vs control and preserved LVEF.

infected with 10^5 (n=14) presented no significant difference in relation to LVEF ($70.7\pm17.6\%$ and $75.8\pm17.9\%$, respectively, $P=0.41$), extent of inflammatory infiltrate (142.4 ± 97.3 nuclei/mm^2 and 141.8 ± 44.6 nuclei/mm^2, $P=0.98$), and WMA score (1.04 ± 0.07 and 1.23 ± 0.38, $P=0.09$), but presented more extensive fibrosis ($9.04\pm3.7\%$ and $5.3\pm2.0\%/mm^2$, $P=0.002$, respectively).

Temporal evolution

When compared to the animals investigated at the time window of 6 months after infection, the animals studied at 10 months after infection presented lower LVEF ($78.4\pm13.6\%$ versus $46.9\pm8.5\%$, respectively, $P<0.0001$), increased LV diastolic diameter (0.49 ± 0.07 cm versus 0.70 ± 0.13 cm, respectively, $P<0.0001$) and higher WMA score (1.04 ± 0.07 versus 1.74 ± 0.49, respectively, $P=0.003$).

The histological analysis showed more severe involvement in the 10-month animals when compared to the 6-month animals, regarding extension of fibrosis ($12.56\pm2.37\%/mm^2$ versus $7.53\pm3.23\%/mm^2$, $P=0.003$) and inflammatory infiltrate (266.2 ± 72.9 nuclei/mm^2 versus 89.4 ± 41.2 nuclei/mm^2, $P<0.0001$).

Discussion

The main results of the present study show that, similarly to what is seen in human CCC, striking WMA despite still-preserved global LV systolic function are detected in a substantial proportion (24%) of the animals in this experi-
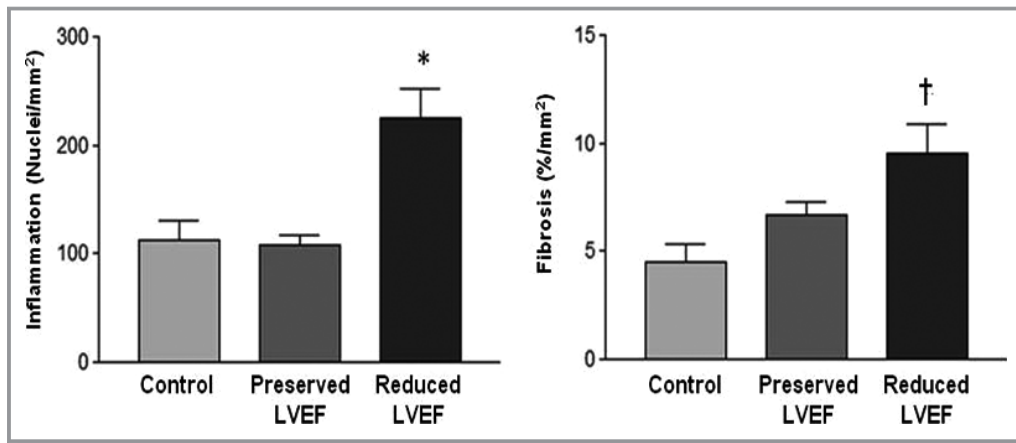
Figure 4. Bar graphs representing the mean values of the quantitative histopathological analysis in the animals classified according to the LV systolic function. The error bars represent SEM. The sample size of each group of animals is the following: control n=7; preserved LVEF n=24; reduced LVEF n=10. *P<0.01 in comparison with control animals and the animals with preserved LVEF; †P<0.05 in comparison with control animals. LVEF indicates left ventricular ejection fraction.

mental model of *T. cruzi* chronic infection. Even more importantly, these areas of regional contractile dyssynergy were more intensely correlated with inflammatory histopathological changes than with the extent of interstitial fibrosis. In addition, the abnormalities in wall motion detected in these infected hamsters were predominant in the same regions usually showing LV regional dysfunction in humans (ie, the apical, and the basal portion of the posterior-lateral and inferior walls).

Global LV Systolic Dysfunction

In this model of chronic *T. cruzi* infection, during a time window of 6 to 10 months after an intraperitoneal inoculum

of 3.5×10^4 to 10^5 infecting forms, a significant portion of the animals (29%) showed global systolic dysfunction and dilation of the LV cavity. These results corroborate those obtained in another study also using the Echocardiogram in the same experimental model,[12] in which 28% of the animals showed ventricular dysfunction associated with dilation and diffuse hypocontractility within a time window of 8 months after infection. In addition, the present data also confirm the evolving nature of the CCC, as the degree of LV remodeling and systolic dysfunction presented a clear worsening at the time window of 10 months after infection as compared to the 6-month evaluation.[10,12]

In the present investigation, qualitative histological analysis showed multifocal myocarditis due to a mononuclear
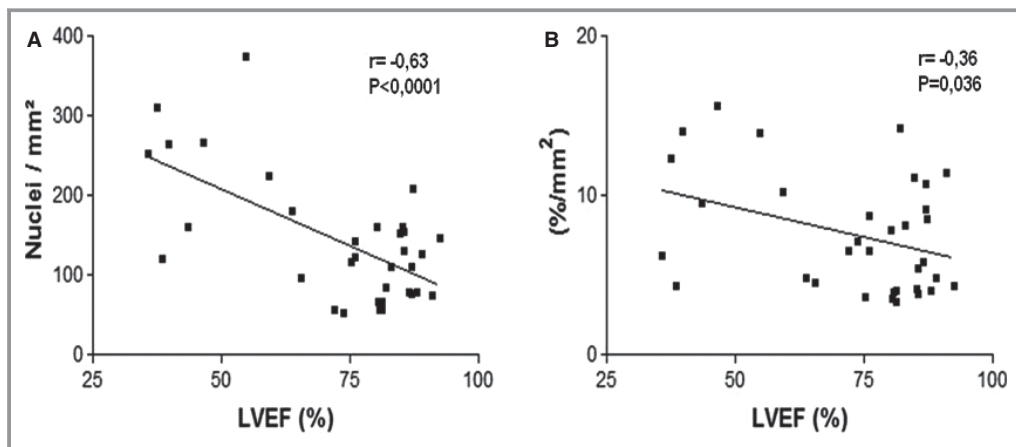

Figure 5. Dispersion plots illustrating the correlation analysis between individual values of LVEF and the intensity of inflammation (A) and extent of fibrosis (B), in the infected animals (n=34). LVEF indicates left ventricular ejection fraction.
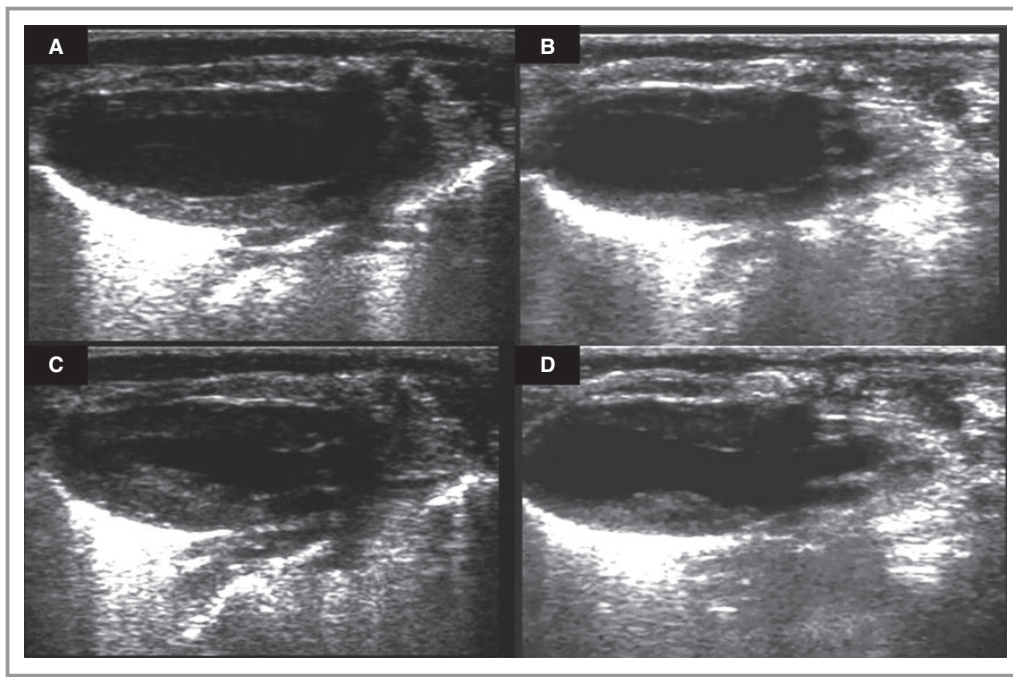
Figure 6. Illustrative echocardiography long-axis images obtained from the parasternal view showing the diastolic and systolic frame of animals of the infected group with normal segmental wall motion (A and B) and with segmental wall motion abnormalities (apical akinesia, C and D).

infiltrate, fiber degeneration, and myocytolytic lesions associated with a mild increase in interstitial and perivascular fibrosis, but without the formation of areas of coalescent fibrosis involving a significant extent of the ventricular wall. The histological changes were more prominent in animals with higher degrees of LV dysfunction, also in agreement with previous descriptions of the histopathological abnormalities occurring in this experimental model of CCC.[10,12]

Quantitative analysis also permitted observation of the correlation between each type of histological abnormality (inflammation or fibrosis) and the degree of global LV systolic dysfunction. Thus, the present results showed a stronger correlation between LVEF and the intensity of inflammation than with the extent of fibrosis. Multiple regression analysis revealed that only inflammation was independently correlated with LVEF when both variables were introduced in the model.

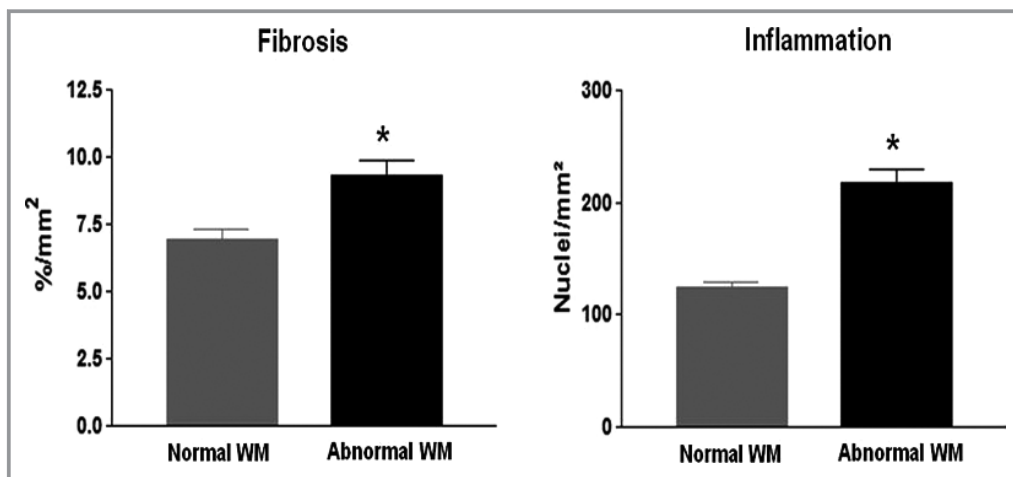**Figure 7.** Bar graphs representing the extent of myocardial fibrosis and inflammation in the segments with normal (n=101 segments) and abnormal wall motion (WM) (n=337 segments) in the same hamsters. The error bars represent SEM. *$P < 0.0001$.

Taken together, these findings indicate that inflammation may participate as a significant mechanism leading to LV systolic dysfunction during the progression of CCC. The notion that inflammation may play a central role in the pathogenesis of CCC has been supported in previous clinical studies using endomyocardial biopsy obtained from patients with various stages of the evolution of the disease, showing that the intensity of inflammation was directly associated with disease severity and that patients with heart failure had a high prevalence of active myocarditis.[19,20] The role of inflammatory mediators such as cytokines (tumor necrosis factor-α, interferon-γ, and chemokines such as CCL2/MCP1 and CXCL9/MIG) in disease progression has been observed. These mediators have been reported to induce pathological remodeling of the heart by inducing changes in gene expression leading to pathological hypertrophy and dilation.[21] Interferon-γ and tumor necrosis factor-α are produced in the myocardium of chronically *T. cruzi*-infected hamsters.[13] CCC patients display abundant myocardial production of tumor necrosis factor-α, interferon-γ, CCL2/MCP1, and CXCL9/MIG.[21–24]

Regional LV Systolic Dysfunction

With this CCC model we detected LV regional wall motion abnormalities as a distinct evidence of chronic myocardial involvement in a significant proportion (24%) of chronically *T. cruzi*-infected animals. This was the first experimental study of small rodents based on in vivo images demonstrating these WMA. For this we took advantage of instrumentation allowing higher-resolution images that was not reported in other studies using the same experimental model.[12,13,25]

Histological analysis based on systematic sampling of LV walls to permit a topographic correlation with the wall motion derangements revealed a greater intensity of inflammation and a larger volume of interstitial and perivascular fibrosis in segments with altered parietal mobility compared to segments with normal wall motion. However, it should be emphasized that the fibrosis found was only mild, not exceeding 10% of the myocardial area and producing no areas of coalescent fibrosis; also, the fibrotic process was not sufficient to have a transmural extension of the ventricular wall that might indicate its direct participation in the reduction of parietal mobility of the segments involved. Thus, the histological analysis suggests that inflammation may be the main component of tissue injury and be more directly involved in the genesis of regional contractile dysfunction in this model of CCC. This concept is additionally supported by the observation that individual LV wall motion score and LVEF values were significantly and independently correlated with a higher intensity of myocardial inflammation. Overall, these results also indicate that the detection of changes in LV regional mobility in animals with still-preserved global function identifies animals exhibiting myocardial damage of a basically inflammatory nature.

Even though this aspect has not been specifically addressed by our study, it is relevant to consider that myocardial perfusion disturbances secondary to microvascular disease could also take part in the pathogenic mechanism causing the regional LV systolic dysfunction in this CCC model.[6,7]

To the best of our knowledge, this is the first experimental study addressing the investigation of the histopathological injuries underlying WMA in CCC. Only one previous study, in rabbits chronically infected with the *T. cruzi*, described LV regional WMA using x-ray contrast ventriculography, but the histopathological analysis showing myocytolytic necrosis, inflammation, and fibrosis was not topographically correlated with those wall motion disturbances.[26]

Topography of the Changes in LV Segmental Parietal Mobility

The present findings agree with data frequently reported in the echocardiography evaluation of patients in the early phases of development of myocardial dysfunction due to CCC, with dyssynergy of the apical region being the most common finding, involving up to 64% of the patients.[16] We also detected WMA in the inferior and posterolateral segments of our animals, again similarly to what is seen in humans, affecting about 30% of all patients.[27,28] The fact that the same myocardial regions are affected both in hamsters and in humans is a considerably intriguing finding whose mechanisms are still unknown.

Implications Regarding CCC in Humans

The present experimental results showing the high incidence of WMA are similar to the reports of various clinical studies showing that regional contractile dysfunction is a characteristic and quite common finding in human CCC, ranging in incidence from 8.5% to 64% in the various series reported in the literature.[16]

The importance of the detection of these regional changes in contractile function is related to what has been shown in clinical studies of patients with areas of regional dyssynergy who have a more marked progression of global LV dysfunction on a medium-term basis compared to patients with CCC without these changes.[17] In addition, the presence of areas of LV dyssynergy is independently correlated with the incidence of LV mural thrombus and is significantly associated with the incidence of cardiovascular events during clinical follow-up.[29–31]

Autopsy studies have shown that the typical aneurysms found in patients with CCC consist of areas of transmural fibrosis and LV wall thinning both in the apical and the posterolateral regions.[32] Based on these observations, the classical concept was formulated that changes in wall motion represent areas with varying degrees of regional parietal fibrosis.

However, no study has addressed the histological substrate associated with regions of less severe dyssynergy such as hypokinesis in patients in the earlier stages of development of myocardial disease with still-preserved LV systolic function. More recently, clinical studies using cardiac magnetic resonance have shown an association between the presence of delayed paramagnetic contrast enhancement, which identifies regions of myocardial fibrosis, with areas of LV wall contractile dyssynergy.[33,34] However, these results also indicate that a relevant proportion of dyssynergic segments were not associated with the presence of delayed enhancement. In a study investigating 67 patients with CCC and various degrees of LV involvement, Regueiro et al detected WMA in 143 myocardial segments, with delayed contrast enhancement occurring in only 93 segments, thus indicating that 35% of the dyssynergic segments showed no detectable LV parietal fibrosis. Scintigraphic studies using severe reduction of thallium uptake as a tool for the identification of regional myocardial fibrosis have also shown that 49% of the dyssynergic segments occur in regions with no defective uptake of the tracer.[35]

Taken together, these results and those from our present study suggest that other mechanisms may be associated with the development of WMA in addition to regional fibrosis. Thus, it is plausible to assume that our experimental results showing that wall motion changes are closely related to the inflammatory damage could be extrapolated to the clinical scenario, and support the hypothesis that myocarditis may be a relevant mechanism causing impaired LV wall motion in humans with early stages of CCC development of myocardial disease despite still-preserved global LV systolic function. One possible corollary is that the control of myocardial inflammation, by using anti-inflammatory drugs, may reduce progression of ventricular dysfunction. On the other hand, since myocarditis is mostly related to parasite persistence, this might have relevant implications regarding the possibility that trypanocidal therapy may benefit patients with early stages of CCC.[36]

Conclusions

Isolated WMA in animals with preserved global systolic LV function are frequently found in Syrian hamsters with experimental CCC whose underlying histopathological lesions are mainly of an inflammatory nature. The topographic distribution of these regional contractile disturbances was similar to that observed in human patients with CCC (ie, are predominant in the apical, inferior, and posterolateral LV segments).

These findings are consistent with the hypothesis that WMA in human CCC may also have an inflammatory basis and not be exclusively due to irreversible fibrotic lesions.

Disclosures

None.

References

1. World Health Organization. *Working to Overcome the Global Impact of Neglected Tropical Diseases: First WHO Report on Neglected Tropical Diseases*. Geneva: World Health Organization; 2010.

2. Bern C, Kjos S, Yabsley MJ, Montgomery SP. *Trypanosoma cruzi* and Chagas' disease in the United States. *Clin Microbiol Rev*. 2011;24:655–681.

3. Paricio-Talayero JM, Benlloch-Muncharaz MJ, Collar-del-Castillo JI, Rubio-Soriano A, Serrat-Pérez C, Magraner-Egea J, Landa-Rivera L, Sánchez-Palomares M, Beseler-Soto B, Santos-Serrano L, Ferriol-Camacho M, Mut-Buigues J, Tomás-Vila M, del Carmen Alonso-Jiménez M, Domínguez-Márquez V, Igual-Adell R. Epidemiological surveillance of vertically-transmitted Chagas disease at three maternity hospitals in the Valencian Community. *Enferm Infecc Microbiol Clin*. 2008;26:609–613.

4. Gascon J, Bern C, Pinazo MJ. Chagas disease in Spain, the United States and other non-endemic countries. *Acta Trop*. 2010;115:22–27.

5. Schmunis GA, Yadon ZE. Chagas disease: a Latin American health problem becoming a world health problem. *Acta Trop*. 2010;115:14–21.

6. Marin-Neto JA, Cunha-Neto E, Maciel BC, Simoes MV. Pathogenesis of chronic Chagas heart disease. *Circulation*. 2007;115:1109–1123.

7. Rossi MA, Carobrez SG. Experimental *Trypanosoma cruzi* cardiomyopathy in BALB/c mice: histochemical evidence of hypoxic changes in the myocardium. *Br J Exp Pathol*. 1985;66:155–160.

8. de Lana M, Chiari E, Tafuri WL. Experimental Chagas' disease in dogs. *Mem Inst Oswaldo Cruz*. 1992;87:59–71.

9. Jelicks LA, Chandra M, Shirani J, Shtutin V, Tang B, Christ GJ, Factor SM, Wittner M, Huang H, Weiss LM, Mukherjee S, Bouzahzah B, Petkova SB, Teixeira MM, Douglas SA, Loredo ML, D'Orleans-Juste P, Tanowitz HB. Cardioprotective effects of phosphoramidon on myocardial structure and function in murine Chagas' disease. *Int J Parasitol*. 2002;32:1497–1506.

10. Ramirez LE, Lages-Silva E, Soares Junior JM, Chapadeiro E. The hamster (*Mesocricetus auratus*) as experimental model in Chagas' disease: parasitological and histopathological studies in acute and chronic phases of *Trypanosoma cruzi* infection. *Rev Soc Bras Med Trop*. 1994;27:163–169.

11. Colmanetti FH, Teixeira Vde P, Rodrigues ML, Chica JE, Reis M, dos Santos VM. Myocardiocyte ultrastructure and morphometrical analysis in hamsters experimentally infected with *Trypanosoma cruzi*. *Ultrastruct Pathol*. 2005;29:139–147.

12. Bilate AM, Salemi VM, Ramires FJ, de Brito T, Silva AM, Umezawa ES, Mady C, Kalil J, Cunha-Neto E. The Syrian hamster as a model for the dilated cardiomyopathy of Chagas' disease: a quantitative echocardiographical and histopathological analysis. *Microbes Infect*. 2003;5:1116–1124.

13. Bilate AM, Salemi VM, Ramires FJ, de Brito T, Russo M, Fonseca SG, Faé KC, Martins DG, Silva AM, Mady C, Kalil J, Cunha-Neto E. TNF blockade aggravates

experimental chronic Chagas disease cardiomyopathy. *Microbes Infect*. 2007;9:1104–1113.

14. Barretto AC, Ianni BM. The undetermined form of Chagas' heart disease: concept and forensic implications. *Sao Paulo Med J*. 1995;113:797–801.

15. de Almeida-Filho OC, Maciel BC, Schmidt A, Pazin-Filho A, Marin-Neto JA. Minor segmental dyssynergy reflects extensive myocardial damage and global left ventricle dysfunction in chronic Chagas disease. *J Am Soc Echocardiogr*. 2002;15:610–616.

16. Acquatella H. Echocardiography in Chagas heart disease. *Circulation*. 2007;115:1124–1131.

17. Pazin-Filho A, Romano MM, Almeida-Filho OC, Furuta MS, Viviani LF, Schmidt A, Marin-Neto JA, Maciel BC. Minor segmental wall motion abnormalities detected in patients with Chagas' disease have adverse prognostic implications. *Braz J Med Biol Res*. 2006;39:483–487.

18. Morgan EE, Faulx MD, McElfresh TA, Kung TA, Zawaneh MS, Stanley WC, Chandler MP, Hoit BD. Validation of echocardiographic methods for assessing left ventricular dysfunction in rats with myocardial infarction. *Am J Physiol Heart Circ Physiol*. 2004;287:H2049–H2053.

19. Pereira Barretto AC, Mady C, Arteaga-Fernandez E, Stolf N, Lopes EA, Higuchi ML, Bellotti G, Pileggi F. Right ventricular endomyocardial biopsy in chronic Chagas' disease. *Am Heart J*. 1986;111:307–312.

20. Higuchi ML, De Morais CF, Pereira Barreto AC, Lopes EA, Stolf N, Bellotti G, Pileggi F. The role of active myocarditis in the development of heart failure in chronic Chagas' disease: a study based on endomyocardial biopsies. *Clin Cardiol*. 1987;10:665–670.

21. Cunha-Neto E, Dzau VJ, Allen PD, Stamatiou D, Benvenutti L, Higuchi ML, Koyama NS, Silva JS, Kalil J, Liew CC. Cardiac gene expression profiling provides evidence for cytokinopathy as a molecular mechanism in Chagas' disease cardiomyopathy. *Am J Pathol*. 2005;167:305–313.

22. Abel LCJ, Rizzo LV, Ianni B, Albuquerque F, Bacal F, Carrara D, Bocchi ED, Teixeira HC, Mady C, Kalil J, Cunha-Neto E. Chronic Chagas' disease cardiomyopathy patients display an increased IFN-gamma response to *Trypanosoma cruzi* infection. *J Autoimmun*. 2001;17:99–107.

23. Nogueira LG, Santos RH, Ianni BM, Fiorelli AI, Mairena EC, Benvenuti LA, Frade A, Donadi E, Dias F, Saba B, Wang HT, Fragata A, Sampaio M, Hirata MH, Buck P, Mady C, Bocchi EA, Stolf NA, Kalil J, Cunha-Neto E. Myocardial chemokine expression and intensity of myocarditis in Chagas cardiomyopathy are controlled by polymorphisms in CXCL9 and CXCL10. *PLoS Negl Trop Dis*. 2012;6:e1867.

24. Nogueira LG, Santos RH, Fiorelli AI, Mairena EC, Benvenuti LA, Bocchi EA, Stolf NA, Kalil J, Cunha-Neto E. Myocardial gene expression of T-bet, GATA-3, Ror-gammat, FoxP3, and hallmark cytokines in chronic Chagas disease cardiomyopathy: an essentially unopposed TH1-type response. *Mediators Inflamm*. 2014;2014:914326.

25. Pimentel Wde S, Ramires FJ, Lanni BM, Salemi VM, Bilate AM, Cunha-Neto E, Oliveira AM, Fernandes F, Mady C. The effect of beta-blockade on myocardial remodelling in Chagas' cardiomyopathy. *Clinics (Sao Paulo)*. 2012;67:1063–1069.

26. Figueiredo F, Marin-Neto JA, Rossi MA. The evolution of experimental *Trypanosoma cruzi* cardiomyopathy in rabbits: further parasitological, morphological and functional studies. *Int J Cardiol*. 1986;10:277–290.

27. Friedman AA, Armelin E, Leme LE, Faintuch JJ, Gansul RC, Diament J, Azul LG. Ventricular performance in Chagas disease. Echocardiographic relations in myocardiopathy with dromotropic disorder and in the preclinical phase. *Arq Bras Cardiol*. 1981;36:23–27.

28. Ortiz J, Barretto AC, Matsumoto AY, Mônaco CA, Ianni B, Marotta RH, Mady C, Bellotti G, Pileggi F. Segmental contractility changes in the indeterminate form of Chagas' disease. Echocardiographic study. *Arq Bras Cardiol*. 1987;49:217–220.

29. Nunes Mdo C, Barbosa MM, Rocha MO. Peculiar aspects of cardiogenic embolism in patients with Chagas' cardiomyopathy: a transthoracic and transesophageal echocardiographic study. *J Am Soc Echocardiogr*. 2005;18:761–767.

30. Carod-Artal FJ, Gascon J. Chagas disease and stroke. *Lancet Neurol*. 2010;9:533–542.

31. Cardoso RN, Macedo FY, Garcia MN, Garcia DC, Benjo AM, Aguilar D, Jneid H, Bozkurt B. Chagas cardiomyopathy is associated with higher incidence of stroke: a meta-analysis of observational studies. *J Card Fail*. 2014;20:931–938.

32. Acquatella H, Schiller NB, Puigbó JJ, Giordano H, Suárez JA, Casal H, Arreaza N, Valecillos R, Hirschhaut E. M-mode and two-dimensional echocardiography in chronic Chages' heart disease. A clinical and pathologic study. *Circulation*. 1980;62:787–799.

33. Rochitte CE, Oliveira PF, Andrade JM, Oliveira PF, Andrade JM, Ianni BM, Parga JR, Avila LF, Kalil-Filho R, Mady C, Meneghetti JC, Lima JA, Ramires JA. Myocardial delayed enhancement by magnetic resonance imaging in patients with Chagas' disease: a marker of disease severity. *J Am Coll Cardiol*. 2005;46:1553–1558.

34. Regueiro A, García-Álvarez A, Sitges M, Ortiz-Pérez JT, De Caralt MT, Pinazo MJ, Posada E, Heras M, Gascón J, Sanz G. Myocardial involvement in Chagas disease: insights from cardiac magnetic resonance. *Int J Cardiol*. 2013;165:107–112.

35. Simoes MV, Pintya AO, Bromberg-Marin G, Sarabanda AV, Antloga CM, Pazin-Filho A, Maciel BC, Marin-Neto JA. Relation of regional sympathetic denervation and myocardial perfusion disturbance to wall motion impairment in Chagas' cardiomyopathy. *Am J Cardiol*. 2000;86:975–981.

36. Marin Neto JA, Sousa AS, Dias JCP, Rassi A. Doença de Chagas: moléstia negligenciada. In: Andrade JPA DK, Pinto FJ, eds. *Tratado de Prevenção Cardiovascular. Um Desafio Global*. Vol. 1. São Paulo: Atheneu; 2014:111–127.